Journal of Science and Technology – Smart Systems and Devices
Volume 36, Issue 2, May 2026, 066–073

Control Design for Overhead Crane with Variable Cable Length

Trinh Vu Dai, Do Trong Hieu*

School of Electrical and Electronic Engineering, Hanoi University of Science and Technology, Ha Noi, Vietnam
**Corresponding author email: hieu.dotrong@hust.edu.vn*

Abstract

Although overhead crane systems play a vital role in industrial operations, their control remains challenging due to underactuated, strong dynamic coupling, and payload oscillations. Existing approaches have shown effectiveness in reducing oscillations but often struggle with external disturbances, parameter variations, and the complexities of tuning. Moreover, many previous studies assume constant payload vibration frequencies, whereas real-world operations frequently involve varying rope lengths, leading to frequency changes and reduced controller performance. To overcome these limitations, this paper proposes a dual control framework: a proportional-derivative and sliding mode control (PD-SMC) strategy for trolley positioning and payload swing suppression, combined with an active disturbance rejection control (ADRC) scheme for cable length regulation. The PD-SMC ensures accurate and robust motion control under disturbances, while ADRC provides fast tracking performance with reduced modeling dependency. Simulation results validate that the proposed approach achieves precise positioning and effective swing suppression, even under varying rope lengths.

Keywords: Crane control design, model uncertainties, swing suppression, underactuated systems, varying rope length.

1. Introduction

Overhead crane systems are essential in numerous industries, providing efficient solutions for material handling and heavy load management. Traditionally, trolley motion and payload lifting are performed sequentially; however, simultaneous control can significantly enhance productivity. A persistent challenge in crane operations lies in payload oscillations, which not only reduce system durability and compromise safety but also make it difficult to achieve precise control of trolley position and cable length. With the growing trend of automation in manufacturing, construction and transportation, the demand for safety, energy efficiency, and high system performance has stimulated increasing interest in advanced control strategies for overhead cranes. Nevertheless, the crane system is basically underactuated, with fewer control inputs than degrees of freedom, and the strong coupling among trolley movement, load swing, and variable cable length further complicates the design of control schemes aimed at achieving fast and accurate motions with minimal oscillations [1].

Extensive studies have been devoted to the control of overhead crane systems, resulting in a variety of strategies for their operation. Among them, open-loop techniques such as input shaping are widely adopted due to their simplicity in design and effectiveness in suppressing load oscillations [2, 3]. However, these methods are generally less capable of compensating for external disturbances. An alternative is output-based command shaping, whose performance, however, depends strongly on both the system order and the selection of the reference model [4, 5]. Most of these studies primarily address the suppression of payload oscillations, whereas in real-world operations cranes are also required to deliver loads to precise target positions. Consequently, this approach is often integrated with a trolley position control loop to ensure accurate load transport [6, 7]. Closed-loop control approaches have been extensively applied in crane systems to mitigate payload oscillations and achieve precise positioning. Methods such as sliding mode control [8] and passivity-based control [9] achieve system stability by exploiting energy-based principles. Although effective, these approaches may face challenges in practical applications due to issues such as sensitivity to parameter variations and modeling uncertainties. Advanced control strategies utilizing the Takagi–Sugeno fuzzy model have also attracted considerable attention [10]. However, their design and parameter tuning are often complicated and require substantial expertise from the designer.

Most previous studies have considered scenarios with time-invariant payload vibration frequencies. In practice, however, cranes often need to transport loads while raising or lowering them simultaneously to enhance efficiency. Such operations cause variations in rope length, which in turn alter the payload's vibration frequency. Consequently, control strategies developed for constant frequencies may prove inadequate when dealing with varying vibration dynamics. To address these challenges, this paper presents a dual control scheme: a proportional-derivative and sliding mode control (PD-SMC) for the trolley position and payload

p-ISSN 3093-3285
e-ISSN 3093-3315
https://doi.org/10.51316/jst.190.ssad.2026.36.2.8
Received: Oct 5, 2025; Revised: Nov 21, 2025;
Accepted: Dec 18, 2025; Online: Jan 14, 2026

swing control, selected due to its effectiveness in minimizing the swing during high-speed motion, and a conventional active disturbance rejection control (ADRC) for the cable length control, which requires less intervention in the load swing but requires fast and accurate tracking. The PD-SMC combines PD control with a sliding mode component to enhance robustness against external disturbances without the need for additional state observers.

The remainder of this paper is structured as follows. Section 2 introduces the dynamic model of a 2D overhead crane system and the proposed control approach. Section 3 provides simulation scenarios and results. Finally, section 4 concludes the paper.

2. Dynamic Model of Overhead Crane Systems and Proposed Control Method

2.1. Dynamic Model

The dynamics of the overhead crane system shown in Fig.1 are given by the following equations [11]:

$$(M+m)\ddot{x}+m\ddot{l}\sin\theta+2m\dot{l}\dot{\theta}\cos\theta - ml\dot{\theta}^2\sin\theta+ml\ddot{\theta}\cos\theta=F_x+F_{rx}-f_x\dot{x} \tag{1}$$

$$(m+m_l)\ddot{l}+m\ddot{x}\sin\theta-ml\dot{\theta}^2-mg\cos\theta = F_l+F_{rl}-f_l\dot{l} \tag{2}$$

$$l\ddot{\theta}+\ddot{x}\cos\theta+2\dot{l}\dot{\theta}+g\sin\theta=0 \tag{3}$$

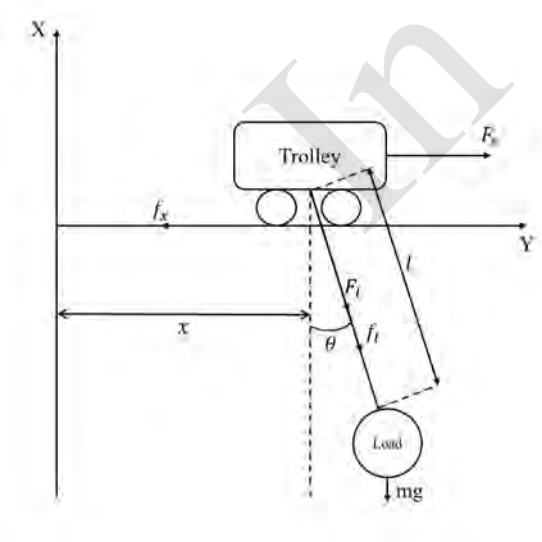

Fig. 1. Schematic illustration of a overhead crane

In the system model, $x(t)$, $\theta(t)$ and $l(t)$ represent the trolley displacement, payload swing angle, and variable rope length, respectively. The control inputs $F_x(t)$ and $F_l(t)$ correspond to the actuating forces applied for trolley motion and for hoisting/lowering operations. The parameters M, m and m_l denote the trolley mass, payload mass and lifting mechanism mass, while g is the gravitational acceleration constant. The terms f_x and f_l represent the viscous friction coefficients associated with trolley translation and rope motion, respectively. F_{rx}, F_{rl} denote the external disturbances acting on the system, respectively.

From (2) and (3), it can be obtained that:

$$\ddot{l}=\frac{-m\ddot{x}\sin\theta+ml\dot{\theta}^2+mg\cos\theta+F_l+F_{rl}-f_l\dot{l}}{m+m_l} \tag{4}$$

$$\ddot{\theta}=-\frac{\ddot{x}\cos\theta+2\dot{l}\dot{\theta}+g\sin\theta}{l} \tag{5}$$

Substituting (4), (5) into (1) we obtain:

$$\left(M+\frac{mm_l\sin^2\theta}{m+m_l}\right)\ddot{x}+\frac{(F_l(t)+F_{rl}-f_l\dot{l})m\sin\theta}{m+m_l} - \frac{mm_l\sin\theta(l\dot{\theta}^2+g\cos\theta)}{m+m_l} = F_x+F_{rx}-f_x\dot{x} \tag{6}$$

To control the position of the trolley to the desired position x_d, the following error signal e is defined as:

$$e=x-x_d \tag{7}$$

From (7), we had the first derivative and the second derivative of the error function as follows:

$$\dot{e}=\dot{x} \tag{8}$$

and

$$\ddot{e}=\ddot{x} \tag{9}$$

From (6) and (9) we obtain:

$$\left(M+\frac{mm_l\sin^2\theta}{m+m_l}\right)\ddot{e}+\frac{(F_l(t)+F_{rl}-f_l\dot{l})m\sin\theta}{m+m_l} - \frac{mm_l\sin\theta(l\dot{\theta}^2+g\cos\theta)}{m+m_l}=F_x+F_{rx}-f_x\dot{x} \tag{10}$$

By introducing a positive constant $\bar{m}$ into (10), (6) can be rewritten as:

$$\begin{aligned}F_x=&\bar{m}\ddot{e}+\left(M+\frac{mm_l\sin^2\theta}{m+m_l}-\bar{m}\right)\ddot{e}\\&+\left(M+\frac{mm_l\sin^2\theta}{m+m_l}-\bar{m}\right)\ddot{x}_d\\&+\frac{(F_l(t)+F_{rl}-f_l\dot{l})m\sin\theta}{m+m_l}\\&-\frac{mm_l\sin\theta(l\dot{\theta}^2+g\cos\theta)}{m+m_l}\\&-F_{rx}+f_x\dot{x}\end{aligned} \tag{11}$$

For simplicity, define P_d as:

$$\begin{aligned} P_d = &\left(M + \frac{mm_l \sin^2\theta}{m+m_l} - \bar{m}\right)\ddot{x}_d \\ &+ \frac{(F_l(t) + F_{rl} - f_l\dot{l})m\sin\theta}{m+m_l} \\ &- \frac{mm_l \sin\theta(l\dot{\theta}^2 + g\cos\theta)}{m+m_l} - F_{rx} + f_x\dot{x} \\ &+ \left(M + \frac{mm_l \sin^2\theta}{m+m_l} - \bar{m}\right)\ddot{e} \end{aligned} \tag{12}$$

Then, (11) can be rewritten as:

$$F_x = \bar{m}\ddot{e} + P_d \tag{13}$$

2.2. Control Law Design for Trolley Position and Payload Swing Reduction

2.2.1. Proposed control law

To reduce the computational burden associated with traditional sliding mode control (SMC) [12], which typically includes two components: the equivalent control term U_{eq} and the switching control term U_{smc}, this study adopts a simplified control strategy. Specifically, the equivalent control component U_{eq} is replaced with a Proportional-Derivative (PD) control law U_{pd}, which is easier to implement and requires less computational effort. To further suppress load swing during trolley movement, an additional control term U_{swing}, which is proportional to the first derivative of the swing angle, is incorporated into the control input.

The sliding surface is selected as:

$$s = e + \alpha\dot{e} \tag{14}$$

where α is a positive coefficient.

Inspired by the control strategy in [13], we propose a modified control law to improve robustness in trolley position control and payload swing reduction:

$$F_x = -(K_p e + K_d\dot{e}) - K_\theta\dot{\theta}^2\dot{e} - K_s\,\mathrm{sign}(s) \tag{15}$$

where K_p and K_d are the proportional and derivative control gains of PD component U_{pd}, K_θ is the gain of stands for the swing-elimination component U_{swing} and K_d is the SMC gain of U_{smc}.

Assumption 1: The payload swing angle follows the condition $-\pi/2 < \theta < \pi/2$.

Assumption 2: For some upper bound constant $\sigma > 0$, the inequality $|\dot{\theta}\ddot{\theta}| < \sigma$ holds.

The PD–SMC law in (15) ensures trolley positioning and reduce payload swing, as detailed below:

$$\lim_{t\to\infty}\begin{bmatrix} x & \dot{x} & \theta & \dot{\theta}\end{bmatrix}^T = \begin{bmatrix} x_d & 0 & 0 & 0\end{bmatrix}^T \tag{16}$$

if the following conditions are satisfied:

$$\begin{cases} K_d > \frac{\bar{m}}{\alpha} \\ K_p > K_\theta\sigma > 0 \\ K_s > \|P_d\| \end{cases} \tag{17}$$

The proof of stability for the proposed PD–SMC method starts with establishing the positive definiteness of the matrix L:

$$L = \begin{bmatrix} K_d & \bar{m} \\ \bar{m} & \alpha\bar{m}\end{bmatrix} \tag{18}$$

From (17), it can be obtained that:

$$\begin{cases} K_d > 0 \\ S = \alpha\bar{m} - \frac{\bar{m}^2}{K_d} > 0 \end{cases} \tag{19}$$

where S is the Schur complement of K_d in L. Then following [13], L is positive definite. The Lyapunov candidate function is defined as:

$$V(t) = \frac{1}{2}\begin{bmatrix} e & \dot{e}\end{bmatrix} L \begin{bmatrix} e \\ \dot{e}\end{bmatrix} + \frac{1}{2}\alpha K_p e^2 + \frac{1}{2}K_\theta\dot{\theta}^2 e^2 \tag{20}$$

Derivative of Lyapunov function $V(e,\dot{e})$ can be easily concluded that:

$$\begin{aligned} \dot{V}(t) = &\begin{bmatrix} e & \dot{e}\end{bmatrix}\begin{bmatrix} K_d & \bar{m} \\ \bar{m} & \alpha\bar{m}\end{bmatrix}\begin{bmatrix}\dot{e} \\ \ddot{e}\end{bmatrix} \\ &+ \alpha K_p e\dot{e} + K_\theta\dot{\theta}^2 e\dot{e} + K_\theta\dot{\theta}\ddot{\theta}e^2 \end{aligned} \tag{21}$$

$$\begin{aligned} = &\begin{bmatrix} e & \dot{e}\end{bmatrix}\begin{bmatrix} K_d\dot{e} + \bar{m}\ddot{e} \\ \bar{m}\dot{e} + \alpha\bar{m}\ddot{e}\end{bmatrix} \\ &+ \alpha K_p e\dot{e} + K_\theta\dot{\theta}^2 e\dot{e} + K_\theta\dot{\theta}\ddot{\theta}e^2 \end{aligned} \tag{22}$$

or

$$\begin{aligned} \dot{V}(t) = &\begin{bmatrix} e & \dot{e}\end{bmatrix}\begin{bmatrix} K_d\dot{e} + F_x - P_d \\ \bar{m}\dot{e} + \alpha\big(F_x - P_d\big)\end{bmatrix} \\ &+ \alpha K_p e\dot{e} + K_\theta\dot{\theta}^2 e\dot{e} + K_\theta\dot{\theta}\ddot{\theta}e^2 \end{aligned} \tag{23}$$

From (14) and (15), we obtain:

$$\begin{aligned} \dot{V}(t) = &s(-P_d - K_s\,\mathrm{sign}(s)) - \big(K_p - K_\theta\dot{\theta}\ddot{\theta}\big)e^2 \\ &- (\alpha K_d - \bar{m})\dot{e}^2 - \alpha K_\theta\dot{\theta}^2\dot{e}^2 \end{aligned} \tag{24}$$

The inequality below is obtained from (17):

$$\begin{aligned} &sK_s\,\mathrm{sign}(s) = \|s\|K_s > \|P_d\|\|s\| \\ &\Rightarrow s(-P_d - K_s\,\mathrm{sign}(s)) \le 0 \end{aligned} \tag{25}$$

$$K_d > \frac{\bar{m}}{\alpha} \Rightarrow (\alpha K_d - \bar{m}) > 0 \tag{26}$$

$$K_p > K_\theta\sigma \Rightarrow K_p - K_\theta\dot{\theta}\ddot{\theta} > 0 \tag{27}$$

Combining conditions (24), (25), (26), and (27), we get the following:

$$\dot{V} \leq 0 \; \forall e, \dot{e} \tag{28}$$

and $\dot{V} = 0$ if and only if $e = 0, \dot{e} = 0$. Since the Lyapunov candidate function V is positive definite and its derivative $\dot{V}(t)$ is negative definite, the overhead crane system under the proposed PD–SMC controller is asymptotically stable. When the state reaches the sliding manifold, the tracking error and its derivative converge asymptotically to zero, in the sense that:

$$e = 0, \dot{e} = 0 \tag{29}$$

From (29) and (14) it can be concluded that:

$$s = 0, e = 0, \dot{e} = 0, \ddot{e} = 0 \tag{30}$$

Substituting the results into (15) yields the following:

$$F_x = 0 \tag{31}$$

In steady state, when the system has converged to the desired position $x = x_d$ and external disturbances are absent $F_{rx} = 0$, assume that the response of the cable length controller is satisfactory in steady state, namely $l = l_d, \dot{l} = 0$, and $F_{rl} = 0$. Then from (2):

$$F_l = -ml\dot{\theta}^2 - mg\cos\theta \tag{32}$$

By using (30), (31), and (32), after some arrangements, (6) can be reduced as:

$$-m\sin\theta(l\dot{\theta}^2 + g\cos\theta) = 0 \tag{33}$$

From Assumption 1, we know that $cos\theta > 0$. Then, it is obtained from (33):

$$sin\theta = 0 \Rightarrow \theta = 0, \dot{\theta} = 0 \tag{34}$$

2.2.2. *Finite-time convergence property of the sliding mode control law*

To complement the asymptotic stability established through the Lyapunov analysis, we now show that the proposed PD–SMC law can guaranty finite-time reaching of the sliding surface.

From (14) and (15):

$$\begin{aligned} \dot{s} &= \dot{e} + \alpha\ddot{e} \\ &= \Delta(t) - \frac{\alpha}{\bar{m}} K_s \text{sign}(s) \end{aligned} \tag{35}$$

where

$$\Delta(t) = \dot{e} - \frac{\alpha}{\bar{m}}\left[K_p e + K_d \dot{e} + K_\theta \dot{\theta}^2 \dot{e} + P_d\right] \tag{36}$$

Assumption 3: There exists a constant $\Delta_{max} > 0$, such that the inequality $|\Delta(t)| \leq \Delta_{max}$ holds $\forall t$.

This assumption is standard because $\Delta(t)$ consists of terms that depend on the bounded variables e, $\dot{e}$, θ, $\dot{\theta}$, and on the disturbance term P_d, which is bounded by design. Consider the Lyapunov candidate:

$$W = \frac{1}{2}s^2 \tag{37}$$

The time derivative of W is given by:

$$\dot{W} = s\dot{s} = s(\Delta(t) - \frac{\alpha}{\bar{m}} K_s \text{sign}(s)) \tag{38}$$

Under the assumption that $|\Delta| \leq \Delta_{max}$, the following inequality holds: $s\Delta(t) \leq |s||\Delta(t)| \leq \Delta_{max}|s|$, which implies:

$$\dot{W} \leq \Delta_{max}|s| - \frac{\alpha}{\bar{m}} K_s |s| = -(\frac{\alpha}{\bar{m}} K_s - \Delta_{max})|s| \tag{39}$$

If we choose
$\frac{\alpha}{\bar{m}} K_s > \Delta_{max}$, then $(\frac{\alpha}{\bar{m}} K_s - \Delta_{max}) = \eta > 0$.

Therefore:

$$\dot{W} \leq -\eta|s| \tag{40}$$

Since $|s| = \sqrt{2W}$:

$$\dot{W} \leq -\eta\sqrt{2W} \text{ or } \frac{\dot{W}}{\sqrt{W}} \leq -\eta\sqrt{2} \tag{41}$$

Then

$$\int_0^T \frac{\dot{W}(t)}{\sqrt{W(t)}} dt \leq \int_0^T -\eta\sqrt{2} dt \tag{42}$$

which implies:

$$2(\sqrt{W(T)} - \sqrt{W(0)}) \leq -\sqrt{2}\eta T \tag{43}$$

Suppose that $s(T) = 0$ then $W(T) = 0$, then from (43) we obtain the finite-time reaching bound:

$$T \leq \frac{\sqrt{2W(0)}}{\eta} = \frac{|s(0)|}{\eta} \tag{44}$$

Consequently, provided Assumption 3 holds, the sliding variable s is driven to $s = 0$ within a finite time T and remains on the sliding surface afterwards.

Since the use of $sign(s)$ in the sliding mode control can lead to chattering, the switching term is modified by replacing $sign(s)$ with the hyperbolic tangent function $\tanh(s)$. This smooth approximation helps reduce chattering while retaining the robustness characteristic of sliding mode control. Note that if a smooth approximation such as $\tanh(s)$ is used instead of $sign(s)$, the result becomes practical finite–time convergence to a small neighborhood of the sliding surface.

Consequently, the modified control input is expressed as follows:

$$F_x = -K_p e - (K_d + K_\theta \dot{\theta}^2)\dot{e} - K_s \tanh(s) \tag{45}$$

2.3. Controller Design for Cable Length

Rewrite (2) in the form:

$$\ddot{l} = f_l + \frac{1}{m+m_l}F_l = f_l + b.F_l \tag{46}$$

where

$$f_l = \frac{-m\ddot{x}\sin\theta + ml\dot{\theta}^2 + mg\cos\theta - F_{rl} + f_l}{m+m_l} \tag{47}$$

Generally, f_l consists of nonlinear terms and uncertain parameters, which are treated as a unified disturbance. Following [14], an Extended State Observer (ESO) is employed to estimate $\hat{f}_l$, thereby compensating for the impact of f_l on the system dynamics by disturbance rejection. The extended state observer is then formulated as follows:

$$\begin{bmatrix}\dot{\hat{x}}_1\\ \dot{\hat{x}}_2\\ \dot{\hat{x}}_3\end{bmatrix} = \begin{bmatrix}-l_1 & 1 & 0\\ -l_2 & 0 & 1\\ -l_3 & 0 & 0\end{bmatrix}\begin{bmatrix}\hat{x}_1\\ \hat{x}_2\\ \hat{x}_3\end{bmatrix} + \begin{bmatrix}0\\ b\\ 0\end{bmatrix}F_l + \begin{bmatrix}l_1\\ l_2\\ l_3\end{bmatrix}l \tag{48}$$

with l_1, l_2, and l_3 representing the ESO parameters, they are determined so that $\hat{x}_1, \hat{x}_2$, and $\hat{x}_3$ provide estimates of $l, \dot{l}$, and f_l, respectively.

Based on the state estimates, the control law is defined as:

$$F_l = \frac{u_0 - \hat{x}_3}{b} \tag{49}$$

where $u_0 = k_p(l_d - \hat{x}_1) - k_d\hat{x}_2$. Substituting (49) into (46) yields:

$$\begin{aligned}\ddot{l} &= f_l - \hat{f}_l + u_0\\ &\approx k_p(l_d - l) - k_d\dot{l}(t)\end{aligned} \tag{50}$$

From (50) we obtain the closed-loop dynamics:

$$\frac{L(s)}{L_d(s)} = \frac{k_p}{s^2 + k_d s + k_p} \tag{51}$$

Given the desired system settling time T_{set}, the parameters are obtained as follows:

$$\begin{cases} s^{CL} \approx \dfrac{-5.85}{T_{\text{set}}}, \quad K_P = (s^{CL})^2, \quad K_D = -2s^{CL}\\ l_1 = -3s^{ESO}, \quad l_2 = 3(s^{ESO})^2, \quad l_3 = -(s^{ESO})^3\\ s^{ESO} = k \cdot s^{CL}, \quad k > 1 \end{cases} \tag{52}$$

3. Simulation Results

To evaluate the effectiveness of the proposed control approach, we compare it with other methods presented in the literature, the H-infinity approach for disturbance rejection in T–S fuzzy systems proposed in [11]. To ensure meaningful comparison, model parameters and simulation scenarios are selected to closely match those in [11], particularly with respect to the trolley position and cable length trajectories. This setup allows us to highlight the advantages of the proposed PD-SMC method more clearly.

In the simulation, the model parameters are adopted from [11] as follows: $M = 5(kg)$, $m_l = 2(kg)$, $m = 0.85(kg)$, $f_x = 20(Ns/m)$, $f_l = 50(Ns/m)$.

To minimize load swing, the input trajectory is designed and used as the reference signal (setpoint). As stated previously, all simulation cases are based on the setup in [11] for consistency. The parameters of the two controllers (PD-SMC and ADRC) are selected as described in Table 1.

Table 1. Parameter of two controller ADRC and PD-SMC

ADRC	Value	PD-SMC	Value
b	$1/(m+m_l)$	α	5.9
k_p	3600	K_p	300
k_d	120	K_d	60
l_1	18.10^2	K_θ	200
l_2	108.10^4	K_s	4
l_3	216.10^5		

We have chosen these following cases in paper [11] to verify the effectiveness of the controller.

- **Case 1:** It aims to evaluate the performance of the proposed controller under nominal conditions without external disturbances. The objective is to move the trolley from the initial position of 0 *m* to 1.5 *m* within 6 *s*, while simultaneously hoisting the load from an initial cable length of 0.6 *m* to 0.2 *m*, and subsequently lowering it back to 0.6 *m*. This scenario is designed to assess the controller's capability in handling coordinated motion of both the trolley and the hoisting mechanism, ensuring smooth trajectory tracking and effective suppression of load swing.

In case 1, the position trajectory and cable length are designed similarly to the reference [11] to ensure a consistent comparison. The proposed controller gives a response closely matching the results reported in [11]as shown in Fig. 2. In particular, the simulated load swing angle indicates that the PD-SMC controller achieves a smaller peak sway angle and significantly reduced oscillations after the trolley reaches the target position, demonstrating improved damping performance.

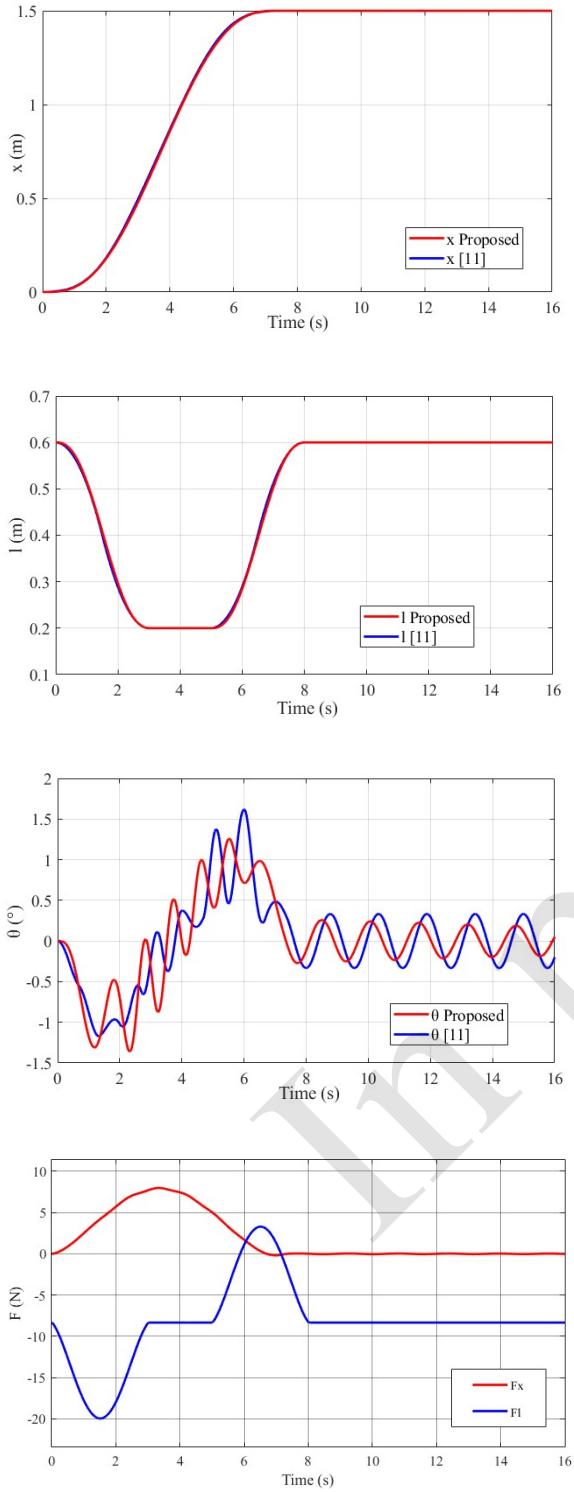

Fig. 2. Case1: Tracking controller without disturbance

- **Case 2:** Scenario maintains the same trolley motion and load hoisting trajectory as described in Case 1. However, in this scenario, external disturbance is introduced into the system to evaluate the robustness of the controller under disturbance conditions. This setup allows for an assessment of the controller's ability to maintain trajectory tracking accuracy and suppress load swing in the presence of external perturbations.

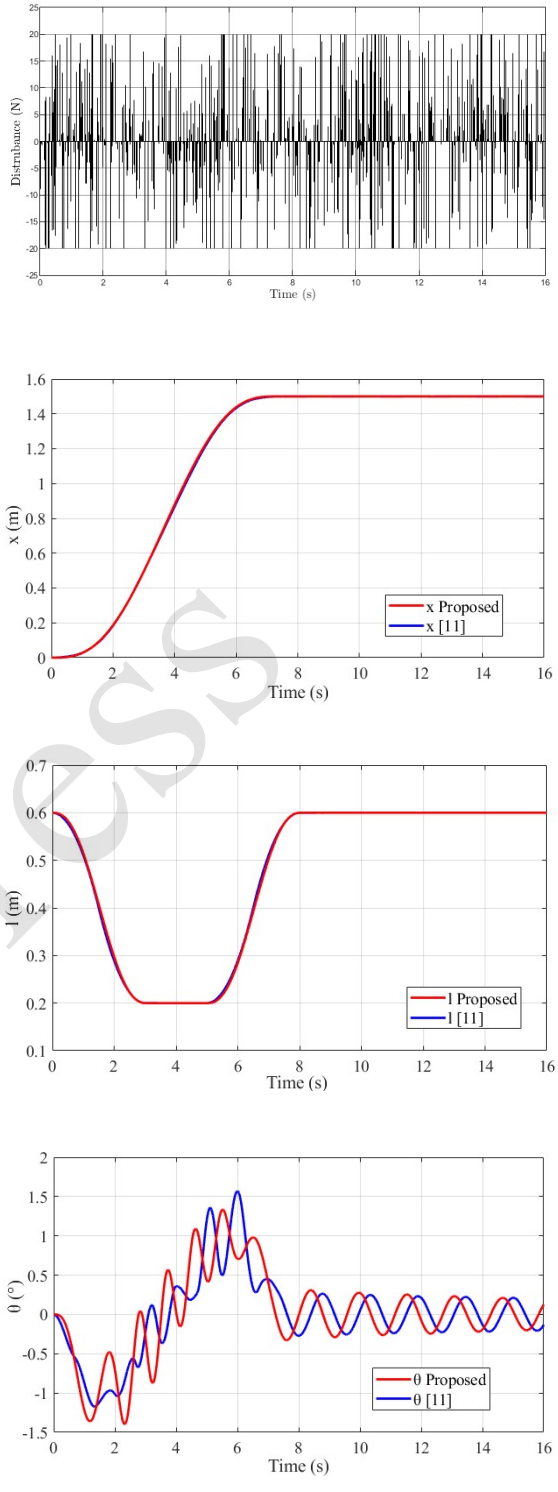

Fig. 3. Case 2: Tracking controller with disturbance with amplitude 20*N*

In Case 2, the setpoints for trolley position and cable length remain unchanged. However, disturbance with an amplitude of 20N is introduced, as shown in Fig. 3 and consistent with the conditions in [11]. Despite the disturbance, the PD-SMC controller maintains effective trajectory tracking performance. Furthermore, the swing angle results demonstrate that the PD-SMC controller outperforms the T–S

fuzzy descriptor approach, exhibiting a notably smaller deviation. In addition, the PD-SMC controller provides well-damped oscillations after the trolley reaches the target position, indicating enhanced robustness against external disturbances.

- **Case 3:** In this case, the model parameters are adopted from [11] as follows: $M = 2(kg)$, $m_l = 0(kg)$, $m = 0.8(kg)$, $f_x = 5(Ns/m), f_l = 5(Ns/m)$. The case aims to evaluates the performance of the proposed controller under ideal conditions without external disturbances. In this scenario, the trolley is required to move from the initial position of 0 m to 2 m within 6 s, while simultaneously lowering the load by extending the cable length from 2 m to 3 m. This test case is designed to verify the controller's ability to handle the downward lifting motion in coordination with the horizontal trolley movement, ensuring smooth trajectory tracking and effective suppression of the load swing.

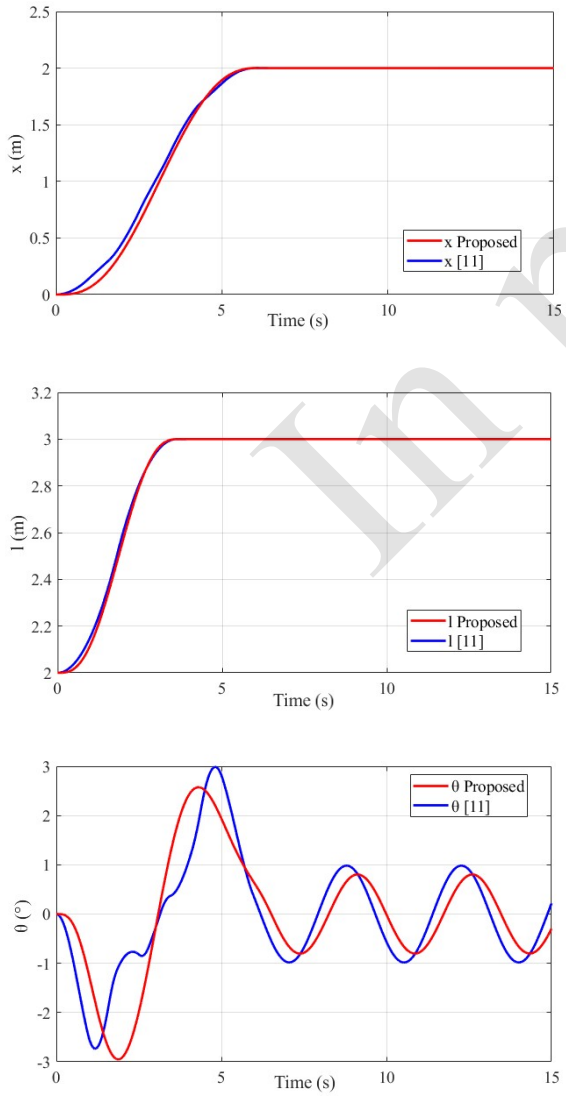

Fig. 4. Case 3: Tracking controller when increasing cable length and trolley position.

In Case 3, we investigate the behavior of the system when both the trolley travel distance, the initial and final cable lengths are increased. The trajectory is designed such that the trolley and hoisting motions reach their setpoints simultaneously. Under these conditions, in Fig. 4 the PD-SMC controller achieves a comparable performance to the control strategy in [11] in terms of trajectory tracking and swing suppression during motion. However, a key distinction is observed in the nature of the load swing. With the PD-SMC controller, the swing angle exhibits a damped response, even without explicitly modeling damping or frictional forces, while the swing response in [11] remains periodic (undamped). This characteristic of the PD-SMC results in a significant reduction in residual oscillations after the trolley reaches its target position, demonstrating improved swing suppression and dynamic stability.

4. Conclusion

This paper has addressed the trajectory tracking problem of a two-dimensional overhead crane system with variable cable length through a hybrid control framework that combines PD-SMC for trolley positioning and ADRC for cable length regulation. In contrast to conventional methods, the proposed scheme integrates oscillation suppression into the PD-SMC law and incorporates trajectory planning to improve tracking accuracy and robustness against disturbances. The simulation results demonstrate that the approach achieves precise positioning, significantly reduces payload swing, and maintains stable performance under varying rope lengths. Although complete elimination of oscillations remains theoretically challenging, the proposed method ensures safe and efficient operation for practical crane applications. Future research will explore the integration of disturbance observers to estimate unmeasured dynamics, thereby enhancing the autonomy and robustness of the system.

Acknowledgement

This research is funded by Hanoi University of Science and Technology (HUST) under project number T2024-PC-062.

References

[1] M. R. Mojallizadeh, B. Brogliato, and C. Prieur, Modeling and control of overhead cranes: A tutorial overview and perspectives, Annual Reviews in Control, vol. 56, pp. 100877, 2023. https://doi.org/10.1016/j.arcontrol.2023.03.002.

[2] M. Maghsoudi, Z. Mohamed, M. Tokhi, A. Husain, and M. Abidin, Control of a gantry crane using input-shaping schemes with distributed delay, Transactions of the Institute of Measurement and Control, vol. 39, no. 3, pp. 361–370, 2017. https://doi.org/10.1177/0142331215607615.

[3] M. Maghsoudi, L. Ramli, S. Sudin, Z. Mohamed, A. Husain, and H. Wahid, Improved unity magnitude input shaping scheme for sway control of an underactuated 3D overhead crane with hoisting, Mechanical Systems and Signal Processing, vol. 123, pp. 466–482, 2019. https://doi.org/10.1016/j.ymssp.2018.12.056.

[4] Z. Mohamed, M. S. Zainal Abidin, S. Buyamin, and A. Bature, Output-based command shaping technique for an effective payload sway control of a 3D crane with hoisting, Transactions of the Institute of Measurement and Control, vol. 39, Apr. 2016. https://doi.org/10.1177/0142331216640871.

[5] A. M. Abdullahi, Z. Mohamed, H. Selamat, H. R. Pota, M. Zainal Abidin, F. Ismail, and A. Haruna, Adaptive output-based command shaping for sway control of a 3D overhead crane with payload hoisting and wind disturbance, Mechanical Systems and Signal Processing, vol. 98, pp. 157–172, 2018. https://doi.org/10.1016/j.ymssp.2017.04.034.

[6] T. B. Tran, M. D. Nguyen, M. D. Duong, and T. H. Do, ZV Shaper – ADRC combination control for crane system with constrained control signal, Journal of Measurement, Control, and Automation, vol. 4, no. 3, pp. 32–38, Dec. 2023. https://doi.org/10.64032/mca.v4i3.189.

[7] M. D. Duong, M. D. Le, D. L. Le, and Q. T. Dao, Control of the Tower Crane Using Input Shaping-Sliding Mode Control, Smart Systems and Devices, vol. 34, no. 1, pp. 51–57, 2024. https://doi.org/10.51316/jst.171.ssad.2024.34.1.7.

[8] M.-S. Park, D. Chwa, and M. Eom, Adaptive sliding-mode antisway control of uncertain overhead cranes with high-speed hoisting motion, IEEE Transactions on Fuzzy Systems, vol. 22, no. 5, pp. 1262–1271, 2014. https://doi.org/10.1109/TFUZZ.2013.2290139.

[9] P.-Y. Shen, J. Schatz, and R. J. Caverly, Passivity-based adaptive trajectory control of an underactuated 3-dof overhead crane, Control Engineering Practice, vol. 112, 2021, Art. no. 104834. https://doi.org/10.1016/j.conengprac.2021.104834.

[10] M.-L. Nguyen, H.-P. Nguyen, and T.-V.-A. Nguyen, H-infinity approach control on Takagi-Sugeno fuzzy model for 2-D overhead crane system, Journal of Applied Science and Engineering, vol. 28, pp. 995–1003, July. 2024. https://doi.org/10.6180/jase.202505 28(5).0008.

[11] H.-P. Nguyen, N.-T. Bui, and T.-V.-Ā. Nguyen, Tracking control based on Takagi-Sugeno fuzzy descriptor model for overhead crane combined with input shaping, IEEE Access, vol. 12, pp. 127507–127521, 2024. https://doi.org/10.1109/ACCESS.2024.3456815.

[12] D. Qian and J. Yi, Hierarchical sliding mode control for underactuated cranes: design, analysis and simulation, Springer Berlin, Heidelberg, 2015.

[13] M. Zhang, Y. Zhang, and X. Cheng, An enhanced coupling PD with sliding mode control method for underactuated double-pendulum overhead crane systems, International Journal of Control, Automation and Systems, vol. 17, no. 6, pp. 1579–1588, 2019. https://doi.org/10.1007/s12555-018-0646-0.

[14] T. H. Do, M. D. Nguyen, and M. D. Duong, A modified ETM shaper for double pendulum crane control with payload hoisting, Journal of Applied Science and Engineering, vol. 28, pp. 1727–1735, 2024. https://doi.org/10.6180/jase.202508 28(8).0010.